

Rainfall rate measurement with a polarimetric radar at an attenuated wavelength

Henri Sauvageot¹ and Frédéric Mesnard

Université Paul Sabatier, Laboratoire d'Aérodynamique, Toulouse, France

Anthony J. Illingworth

University of Reading, U.K.

John W. F. Goddard

Rutherford Appleton Laboratory, U.K.

Abstract. Among the many ways investigated for radar estimation of rainfall, polarimetric methods are the most promising. However most polarimetric algorithms are degraded by attenuation by precipitation and clouds and by calibration error. A new method was recently proposed in which the differential polarimetric attenuation is used to perform an accurate rain rate measurement. The method is independent of the radar calibration and of the attenuation by undetected clouds. This algorithm is also usable as a qualitative hail detector, as well as a detector of anomalous propagation. The goal of the paper is to describe the results of the first experimental implementation of this method using the 35 GHz RABELAIS radar, as attenuated radar, and the 3 GHz CAMRa radar as a reference. We show that the proposed algorithm is stable and enables us to retrieve the actual rain rate even from an observed signal attenuated by more than 30 dB. The results are insensitive to the value used for the power coefficient of the Z(R) relation.

Introduction

Precipitation measurement is the main application of meteorological radar. In most of the radar networks that cover most of the mid-latitude countries (e.g., NEXRAD in USA or ARAMIS in France) and parts of the tropics, the method used to retrieve the rain rate R from the radar-measured reflectivity factor Z is based on a simple power relation of the form:

$$Z = aR^b \quad (1)$$

where a and b are coefficients [e.g., *Joss and Waldvogel*, 1990]. It is known that this algorithm is very inaccurate owing to the dependency of the a and b coefficients on many terms, the main ones of which are storm type and structure, distance from the radar, uncertainty on radar calibration and uncorrected attenuation [*Joss and Waldvogel*, 1990]. All these sources of error are not easily corrected.

To increase the accuracy of rain rate retrieval, many methods more sophisticated than the Z(R) algorithm have been proposed and tested [see review by *Joss and Waldvogel*, 1990; *Sauvageot*, 1994]. At the present time, the most attractive and most investigated methods are the polarimetric ones. They are based on

the observation that larger raindrops are increasingly oblate. The various polarimetric algorithms as well as the techniques to correct their weaknesses and to optimize their implementation are discussed in numerous papers [e.g., *Bringi and Hendry*, 1990 or *Jameson*, 1991]. Many of these methods are derived from the algorithm pioneered by *Seliga and Bringi* [1976] using the measurement of the differential reflectivity, Z_{DR} , that is the ratio of the diagonal terms of the backscattering matrix Z_{HH}/Z_{VV} where the subscripts H and V stand for horizontal and vertical linear polarization. However, these algorithms are also affected by several sources of error, mainly: the uncertainty of the radar calibration, spatio-temporal variability of the drop size distribution (DSD), hail contamination, and, at shorter wavelengths than S-band, atmospheric attenuation. This last term is the sum of two components: attenuation by rain, that can be corrected when low but not when strong [*Hildebrand*, 1978], and attenuation by water clouds, which is frequently ignored, even when it is not at all negligible, notably for ground-based radar, at long distance, and for airborne radar, including when using space diversity algorithms as shown by *Lin Tian and Srivastava* [1997]. For example at X-band, a water cloud with a water content of 2 g m^{-3} produces the same attenuation as rain of about 11 mm h^{-1} [*Sauvageot*, 1992, p. 149 and 231].

Algorithms using the specific differential phase K_{DP} , recently proposed, are less sensitive to DSD variations and not affected by attenuation and by radar calibration [*Jameson*, 1985; 1991; *Sachidananda and Zrnich*, 1987; *Goddard et al.*, 1994; *Ryzhkov and Zrnich*, 1996; *Zrnich and Ryzhkov*, 1996]. However, K_{DP} is very noisy at low rain rates and, therefore light rain rate estimates are not reliable [*Chandrasekar et al.*, 1990; *Kostinski*, 1994].

Sauvageot [1996] proposed an algorithm for rain rate measurement with a polarimetric radar working at an attenuated wavelength. Theoretical arguments and numerical simulation show that this algorithm is: independent of radar calibration, weakly influenced by the shape of the DSD, not biased by the attenuation by water clouds and able to qualitatively detect anomalous propagation and the presence of hail in the rain shaft. *Sauvageot* [1996] presents numerical simulations supporting the validity of his algorithms, but no implementation on field measurement.

The object of this paper is, after a brief review on the attenuated polarimetric algorithm, to present the first example of results from real data.

The attenuated polarimetric method

The schematic of the attenuated polarimetric method (APM) is summed up in Figure 1a [see *Sauvageot*, 1996; for details]. We consider the single polarization radar reflectivity factor, Z_H , and

¹ Corresponding author address: Dr. Henri Sauvageot, Université Paul Sabatier, Observatoire Midi-Pyrénées, Laboratoire d'Aérodynamique, 14 avenue Edouard Belin, 31400 Toulouse, France. e-mail: sauh@aero.obs-mip.fr

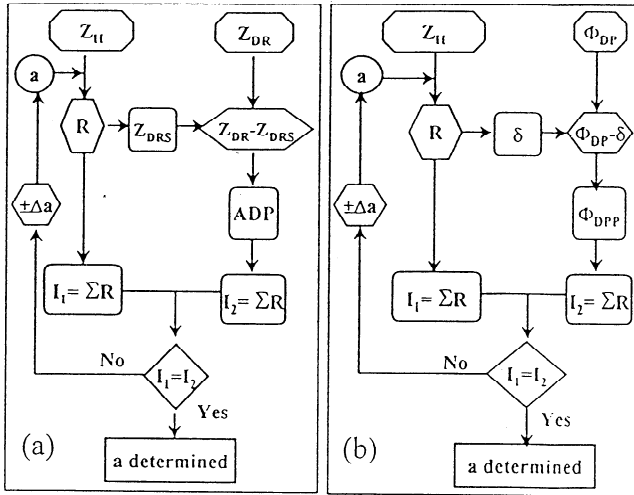


Figure 1. Schematic of the Attenuated Polarimetric Method. *a* is the linear coefficient of the Z-R relation, γ is the power coefficient of the A(R) relation where A is the single polarization attenuation coefficient of rain. a) with the differential reflectivity, b) with the differential phase shift.

the differential reflectivity for horizontal and vertical polarization, Z_{DR} , observed with an attenuated wavelength radar. At attenuated wavelengths, Z_{DR} is the addition of a term depending on the drop shape, Z_{DRS} , and a term depending on the differential attenuation for the two polarizations, A_{DP} . The differential attenuation can be interpreted as an estimation of the integral of the rain rate along the radar beam. A_{DP} is weakly sensitive to DSD. The principle of the method is the following: a first estimation of the rain rate R is calculated from Z_H using the usual step by step iterative attenuation correction scheme [Hildebrand, 1978]. To apply this algorithm, we use a combination of a $Z(R)$, eq.(1), and an $A(R)$ relation of the form:

$$A(R) = kR^\gamma \quad (2)$$

where A is the single polarization attenuation coefficient in rain and k and γ are coefficients. We know the coefficients of the $A(R)$ relation for the used wavelength but we do not know the a and b coefficients of the $Z(R)$ relation. We decide that b will be kept constant at the mean climatological value and that a will be the variable (adjustable) factor. This computation produces I_1 , a summation along the ray path of R . I_1 is false due to the uncertainty in a . Then we consider the cumulative value of the attenuated Z_{DR} observed at the end of the ray path (or at the end of a segment of the ray path). From R , using an assumed DSD, we compute Z_{DRs} , that is the (unattenuated) Z_{DR} , only depending on the drop shapes. The difference between Z_{DR} (observed) and Z_{DRs} (calculated) produces A_{DP} , the polarimetric differential attenuation. From A_{DP} , using again the $A(R)$ relation, we compute I_2 , another summation of R along the ray path. I_2 is false due to the uncertainty on Z_{DRs} , that is on a . Then, we write that I_1 has to be equal to I_2 , that is that the data have to be self-consistent. If I_1 is different from I_2 , we modify a by Δa and run again the I_1 and I_2 computation. When $I_1 = I_2$, the fitted a is determined and we use it in a $Z(R)$ relation to retrieve the corrected R distribution in each range gate.

The ray path observed with the radar can be partitioned and the algorithm applied independently to the individual segments, with one value of a computed for each segment. Of course, usually, at the beginning of the computation, the step by step attenuation

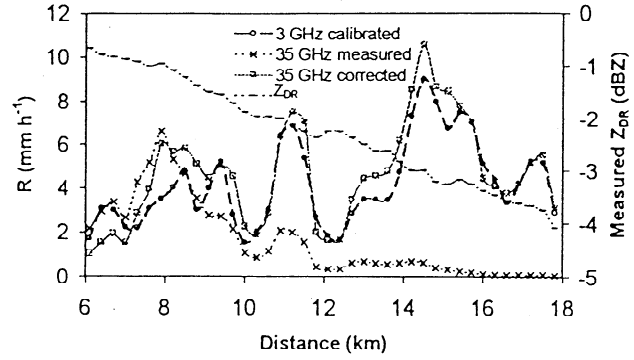


Figure 2. Rain rate R as a function of distance observed with the calibrated 3 GHz radar, with the attenuated 35 GHz radar and retrieved from 35 GHz using the APM with 8 iterations. Measured Z_{DR} is also shown (vertical scale on the right).

correction scheme [Hildebrand, 1978] is not convergent, but this does not raise difficulty since what is needed is only the sign of $I_1 - I_2$. To compute a , we can use, for example, a "dichotomy", a well-known numerical technique.

Of course, with X, C and S band radars, with heavy rainfall, Z_{DR} can be replaced, in the APM, by ϕ_{DP} , the differential phase shift (Fig. 1b). ϕ_{DP} is the sum of two terms, ϕ_{DPP} , the (range cumulative) differential propagation phase shift and δ , the differential backscatter phase shift. For the three bands, ϕ_{DPP} is nearly linearly related both to the attenuation and differential attenuation as shown by Brangi et al. [1990]. Thus ϕ_{DPP} , like A_{DP} , is able to produce I_2 . To obtain ϕ_{DPP} , ϕ_{DP} has to be corrected for δ . Now δ can be estimated from Z and Z_{DRS} [Scarchilli et al., 1993].

In order to minimize the value of Z_{DRS} or δ , it is preferable to use, for Z_{DR} or ϕ_{DP} measurement, range gates where the reflectivity is as low as possible (that is the range gates located behind the rain cell cores).

Data

The correct way to test this algorithm consists in measuring rain rates and cumulative rain heights, using only a polarimetric attenuated radar, and in comparing the results with independent data obtained at the ground with a raingauge network. Such an experiment will be implemented in the near future with an X-band radar in France. A first attempt at verifying this method on

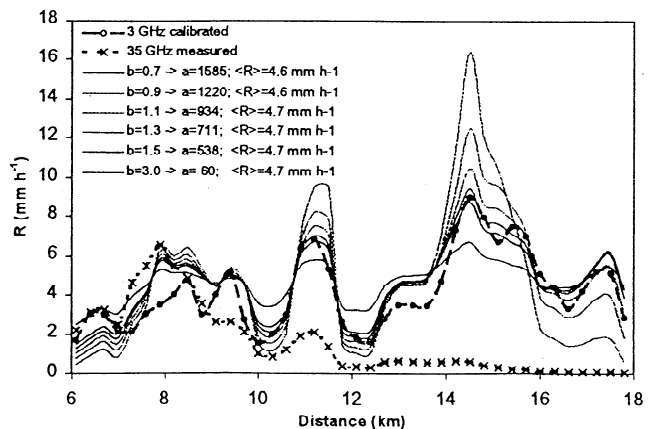


Figure 3. The same as Figure 2 for various values of b . The corresponding a are given, as well as $\langle R \rangle$, the average rain rate computed between 6 and 18 km.

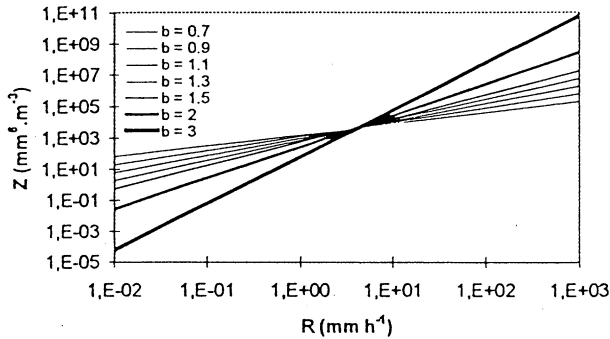


Figure 4. Curves $Z = aR^b$ for the various couples (a_i, b_i) of Figure 3. All the curves intersect at the point corresponding to $R \cong 4.02 \text{ mm h}^{-1}$.

real data was performed on the site of the Chilbolton radar observatory (Rutherford Appleton Laboratory) in UK, using two radars: 1) the Ka band (35 GHz) polarimetric Doppler radar RABELAIS as attenuated radar working with the APM and 2) the unattenuated S band (3 GHz) polarimetric Doppler radar CAMRa, regularly calibrated against raingauges, as a reference. 35 GHz is a very poor frequency for rainfall measurement both because, for that frequency, almost all the size range of raindrops are out of the Rayleigh scattering region and because of heavy attenuation by precipitation. On the other hand, at 35 GHz, the variation of Z_{DR} with R is not wide and so Z_{DR} is not strongly influenced by DSD, what is favorable to the APM implementation. Also, at Ka band frequencies, ϕ_{DP} is almost independent of R . Thus the ϕ_{DP} side of the APM cannot be tested. The 0.41° beamwidth Ka band antenna is set on the side of the 0.25° beamwidth S band antenna enabling a direct ray by ray comparison (see *Goddard et al.*, [1995] where the technical characteristics of the radars are given). For CAMRa, owing to the huge antenna, the near-field area ranges up to about 6 km from the radar.

Results

Figure 2 presents the case observed on July 26, 1995 at 0846 UTC. The curves show the average over three contiguous radii with an azimuth between $69^\circ 40'$ and $70^\circ 20'$ and for a 0° elevation. The object of this averaging is to reduce a possible mismatching of the two radar beams due to the different beamwidths and to the side by side position. The range gates are

0.3 km from each other with the analysis starting at a distance of 6 km (end of the near-field zone). Three curves are presented showing the rainfall rate R as a function of the distance. A fourth curve shows the measured Z_{DR} versus distance. The dashed line (with the open circles) is the rain rate observed with the 3 GHz radar calibrated against raingauges. The dotted line (with crosses) is the rain rate observed with the 35 GHz radar. What can be seen is that the Ka band measurement is strongly attenuated in the first rain cell, between 6 and 10 km. Beyond 10 km, the information on the R distribution is ruined. After 16 km the signal is almost at extinction, the inferred R is 0.1 and 0.05 mm h^{-1} at 16 km and at 17.8 km respectively. The unbroken line (with open squares) displays the 35 GHz rain rate after processing with the APM, without using any other piece of information. Some discrepancies with the 3 GHz rain rate are observed before 10 km (possibly due to beams mismatch). Beyond 10 km the attenuated polarimetric algorithm almost exactly retrieves the observation of the 3 GHz radar. The attenuation corrected by the APM at the end of the line is larger than 30 dB (from 0.05 to 4 mm h^{-1} that is, in terms of reflectivity factor, from about 2 dBZ to 34 dBZ).

For the computation, we have used $b = 1.1$. This is the value computed by *Wexler and Atlas* [1963] at 35 GHz for Mie scattering and exponential DSD at 0°C . The average of the a coefficient obtained using the APM in the case of Figure 2 is 934 (the three individual values are 962, 948 and 892). This value is almost two times that computed by *Wexler and Atlas* [1963] which is 450 for R between 5 and 20 mm h^{-1} .

Figure 3 is a test on the sensitivity of the APM algorithm to the condition $b = \text{constant}$. Using the same case as in Figure 1, b was varied from 0.7 to 3.0 in steps of 0.2 up to 1.5. The curves and the a values computed with the APM for each b appear in Figure 3. The corresponding $Z(R)$ curves (equation 1) are shown in Figure 4. What can be seen in Figure 4 is that all the $Z(R)$ curves intersect at the same point of abscissa $R \cong 4.0 \text{ mm h}^{-1}$. This point is close to $R = \langle R \rangle$, the value of the rain rate averaged along the ray path. This behavior of the couple (a, b) conveys the condition $I_1 = I_2$ with I_2 not dependent on a or b . Whatever the value prescribed for b , the couple (a, b) , determined from the algorithm, has to be such that the constraint provided by A_{DP} is satisfied. This constraint from the cumulative differential attenuation is equivalent to a constraint on $\langle R \rangle$ along the considered segment of the ray path. In the present case (Figure 3), we found that, between 6 and 18 km of distance, $\langle R \rangle \cong 4.6 \text{ mm h}^{-1}$.

If (a_0, b_0) is the optimal couple of the $Z(R)$ coefficients, when b_i is larger than b_0 , the computed value for a_i is smaller than a_0 and the curve $R_i(r)$, where r is the distance (as in Figures 2 and 3), is above $R_0(r)$ for $R_0(r) < \langle R \rangle$ and below $R_0(r)$ for $R_0(r) > \langle R \rangle$.

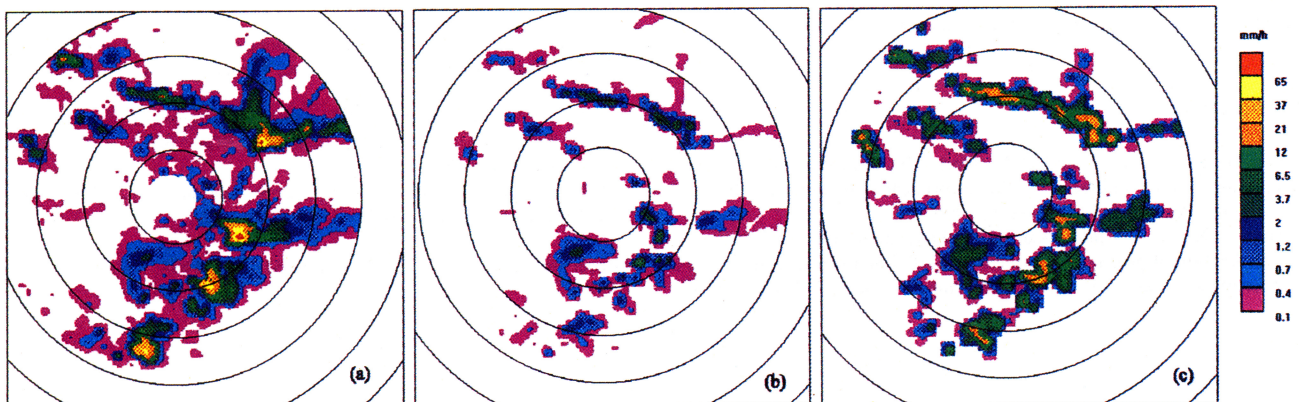


Figure 5. Distribution of the rain rate for an azimuthal scan at elevation of 0° , observed on 12 September 1995 at 1203 UTC, a) with the calibrated 3 GHz radar, b) with the strongly attenuated 35 GHz radar and c) retrieved from the 35 GHz radar data using the APM. Range markers are 10 km from each other.

Table 1. Cumulative value H of the rain rate for the azimuthal scan of Figure 6. The observed area A_0 is the annular area between the distance 6 km and r .

r (km)	uncorrected 35 GHz (mm h ⁻¹)	calibrated 3 GHz (mm h ⁻¹)	Retrieved with APM from 35 GHz (mm h ⁻¹)
$r = 20$	255	1476	1389
$r = 30$	491	3097	3379
$r = 40$	538	4001	3987

It is the opposite for b_i smaller than b_0 . In addition, Figure 3 shows that the amplitude of the fluctuations of $R_i(r)$ around the average $\langle R \rangle$, that is $|R_i(r) - \langle R \rangle|$ decreases when b increases. This behavior conveys the fact that the derivative dR/db is proportional to b^{-2} .

On Figure 3, the computed values of $\langle R \rangle$ for each couple (a_i, b_i) are specified, confirming that $\langle R \rangle$ is not at all affected by the choice of b prescribed for the computation. This finding justifies in part, a posteriori, the condition $b = \text{constant}$ used in the APM.

This ability of the APM to estimate $\langle R \rangle$ is notably interesting for the implementation of the estimation of rainfall by the area integral methods [Doneaud *et al.*, 1984; Atlas *et al.*, 1990].

Figure 5 shows the results of using the APM for the processing of an azimuthal scan in a rain field. Figures 5 a, b and c are the field of rain rate measured with the calibrated 3 GHz radar, observed with the 35 GHz radar and retrieved from the 35 GHz data of b using the APM, respectively. What can be seen is that, in each pixel where the 35 GHz radar detects a signal, a rain rate similar to the 3 GHz radar value is retrieved. Careful examination shows that, on Figure 5c, the peak values are slightly underestimated and the background rain is overestimated, what suggest that $b = 1.1$ is a bit higher than the actual b . The cumulative R for all the azimuthal scan of Figure 5 (that is $H = \sum R_{ij}$ where i, j are the pixel coordinates) and for r (the maximal observed distance) varying between 20 and 40 km obtained in the observed area A_0 (the annular area between the distances 6 km and r), with the 3GHz radar, with the (uncorrected) 35 GHz radar and retrieved from the APM with the 35 GHz data are given in Table 1. Clearly, the APM is a promising method.

Conclusion

The APM is able to retrieve the rain rate distribution as long as the radar signal is above the extinction level.

The $\langle R \rangle$ computed from the APM is insensitive to the value used for b , the power coefficient of the $Z(R)$ relation.

References

Atlas, D., D. Rosenfeld, and D.A. Short, The estimation of convective rainfall by area integrals, 1, the theoretical and empirical basis, *J. Geophys. Res.*, 95, D3, 2153-2160, 1990.
 Bringi, V.N., V. Chandrasekar, N. Balakrishnan and D.S. Zrnice, An examination of propagation effects in rainfall on radar measurements at microwave frequencies, *J. Atmos. Oceanic Technol.*, 7, 829-840, 1990.

Bringi, V.N., and A. Hendry, Technology of polarization diversity radars for meteorology, in *Radar in Meteorology*, D. Atlas, editor, Amer. Meteor. Soc., Boston, 153-190, 1990.
 Chandrasekar, V., V.N. Bringi, N. Balakrishnan, and D.S. Zrnice, Error structure of multiparameter radar and surface measurements of rainfall. Part III: Specific differential phase, *J. Atmos. Oceanic Technol.*, 7, 621-629, 1990.
 Doneaud, A.A., S.I. Niscov, D.L. Priegnitz, and P.L. Smith, The area-time integral as an indicator for convective rain volumes, *J. Appl. Meteor.*, 23, 555-561, 1984.
 Goddard, J.W.F., K.L. Morgan, A.J. Illingworth, and H. Sauvageot, Dual-wavelength polarisation measurements in precipitation using the CAmRa and RABELAIS radars, *Prep. 27th Radar Meteor. Conf.*, Vail, Amer. Meteor. Soc., Boston, 196-198, 1995.
 Goddard, J.W.F., J. Tan and M. Thurai, Technique for calibration of meteorological radars using differential phase, *Electronics Lett.*, 30, 166-167, 1994.
 Hildebrand, P.H., Iterative correction for attenuation of 5 cm radar in rain, *J. Appl. Meteor.*, 17, 508-514, 1978.
 Jameson, A.R., Microphysical interpretation of multi-parameter radar measurements in rain. Part III: Interpretation and measurement of propagation differential phase shift between orthogonal linear polarization, *J. Atmos. Sci.*, 42, 607-614, 1985.
 Jameson, A.R., A comparison of microwave techniques for measuring rainfall, *J. Appl. Meteor.*, 30, 32-54, 1991.
 Joss, J., and A. Waldvogel, Precipitation measurement and hydrology, in *Radar in Meteorology*, D. Atlas, editor, Amer. Meteor. Soc., Boston, 577-606, 1990.
 Kostinski, A.B., Fluctuations of differential phase and radar measurements of precipitation, *J. Appl. Meteor.*, 33, 1176-1181, 1994.
 Lin Tian, and R.C. Srivastava, Measurement of attenuation at C band in a convective storm by a dual-radar method, *J. Atmos. Oceanic Technol.*, 14, 184-196, 1997.
 Ryzhkov, A.V., and D.S. Zrnice, Assessment of rainfall measurement that uses specific differential phase, *J. Appl. Meteor.*, 35, 2080-2090, 1996.
 Sachidananda, M., and D.S. Zrnice, Rain rate estimated from differential polarization measurements, *J. Atmos. Oceanic Technol.*, 4, 588-598, 1987.
 Sauvageot, H., *Radar Meteorology*, Artech House, 366 pp., 1992.
 Sauvageot, H., Rainfall measurement by radar: a review, *Atmos. Res.*, 35, 27-54, 1994.
 Sauvageot, H., Polarimetric radar at attenuated wavelengths as a hydrological sensor, *J. Atmos. Oceanic Technol.*, 13, 630-637, 1996.
 Scahilli, G., E. Gorgucci, V. Chandrasekar and T.A. Seliga, Rainfall estimation using polarimetric techniques at C-band frequencies, *J. Appl. Meteor.*, 32, 1150-1160, 1993.
 Seliga, T.A., and V.N. Bringi, Potential use of radar differential reflectivity measurements at orthogonal polarizations for measuring precipitation, *J. Appl. Meteor.*, 15, 69-76, 1976.
 Wexler, R., and D. Atlas, Radar reflectivity and attenuation of rain, *J. Appl. Meteor.*, 2, 276-280, 1963.
 Zrnice, D.S., and A.V. Ryzhkov, Advantages of rain measurements using specific differential phase, *J. Atmos. Oceanic Technol.*, 13, 454-464, 1996.

H. Sauvageot and F. Mesnard, Laboratoire d'Aérodynamique, OMP, 14 avenue Edouard Belin, 31400 Toulouse, France (e-mail: sauh@aero.obs-mip.fr and mesf@aero.obs-mip.fr)

A.J. Illingworth, University of Reading, Department of Meteorology, 2 Earley Gate, PO Box 243, Reading RG6 6BB, UK (e-mail: a.j.illingworth@reading.ac.uk)

J.W.F. Goddard, Rutherford Appleton Laboratory, Chilton Didcot, OX11 0QX, UK (e-mail: j.w.f.goddard@rl.ac.uk)

(Received December 15, 1997; revised May 19, 1998; accepted June 26, 1998.)